Author Manuscript

Author Manuscript

Author Manuscript

Author Manuscript

HHS Public Access

Author manuscript

Exp Dermatol. Author manuscript; available in PMC 2017 December 01.

Published in final edited form as:

Exp Dermatol. 2016 December ; 25(12): 969–976. doi:10.1111/exd.13108.

Fn14 deficiency protects lupus-prone mice from histological lupus erythematosus-like skin inflammation induced by ultraviolet light

Jessica Doerner, MS[1], **Samantha A. Chalmers, MS**[1], **Adam Friedman, MD**[2], and **Chaim Putterman, MD**[1,3]

[1]The Department of Microbiology and Immunology, Albert Einstein College of Medicine, Bronx, NY, USA

[2]Department of Dermatology, George Washington University School of Medicine & Health Sciences, Washington, D.C., USA

[3]Division of Rheumatology, Albert Einstein College of Medicine, Bronx, NY, USA

Abstract

The cytokine TWEAK and its receptor Fn14 are involved in cell survival and cytokine production. The TWEAK/Fn14 pathway plays a role in the pathogenesis of spontaneous cutaneous lesions in the MRL/lpr lupus strain; however, the role of TWEAK/Fn14 in disease induced by ultraviolet B (UVB) irradiation has not been explored. MRL/lpr Fn14 knockout (KO) were compared to MRL/lpr Fn14 wild-type (WT) mice following exposure to UVB. We found that irradiated MRL/lpr KO mice had significantly attenuated cutaneous disease when compared to their WT counterparts. There were also fewer infiltrating immune cells (CD3+, IBA-1+, and NGAL+) in the UVB-exposed skin of MRL/lpr Fn14KO mice, as compared to Fn14WT. Furthermore, we identified several macrophage-derived proinflammatory chemokines with elevated expression in MRL/lpr mice after UV exposure. Depletion of macrophages, using a CSF-1R inhibitor, was found to be protective against the development of skin lesions after UVB exposure. In combination with the phenotype of the MRL/lpr Fn14KO mice, these findings indicate a critical role for Fn14 and recruited macrophages in UVB-triggered cutaneous lupus. Our data strongly suggest that TWEAK/Fn14 signaling is important in the pathogenesis of UVB-induced cutaneous disease manifestations in the MRL/lpr model of lupus, and further support this pathway as a possible target for therapeutic intervention.

Address correspondence and reprint requests to: Chaim Putterman, MD, Division of Rheumatology, Albert Einstein College of Medicine, F701N, 1300 Morris Park Ave., Bronx, NY 10461, USA, Phone: (718) 430-4266, chaim.putterman@einstein.yu.edu.

Author contributions

JD performed most of the experiments, analyzed the data, and wrote the initial draft of the manuscript. SC assisted with mice handling and experimentation. AF analyzed the skin histopathology and contributed to writing the manuscript. CP designed the study, supervised the experiments, and contributed to writing the manuscript.

Conflicts of Interest

The authors report no conflicts of interest.

Author Manuscript Author Manuscript Author Manuscript Author Manuscript

Keywords

Cutaneous Lupus; Photosensitivity; MRL-lpr/lpr; TWEAK; macrophages

Introduction

The skin is commonly affected in systemic lupus erythematosus (SLE), with over 80% of patients having skin manifestations (1–3). Indeed, 4 of 11 criteria used to diagnose SLE are related to cutaneous disease (4). The morphology of cutaneous lupus erythematosus (CLE) varies greatly, and can be classified into acute, subacute, and chronic categories (5).

The MRL/lpr mouse is a spontaneous model of SLE that is commonly used to study various end-organ pathologies, including cutaneous disease (6,7). MRL/lpr mice have a *fas* mutation that leads to defective apoptosis, causing anti-nuclear autoimmunity, lymphadenopathy, glomerulonephritis, and skin disease. The morphology and other key features of cutaneous involvement share several characteristics with the human disease (7,8), including sensitivity to irradiation (9).

Among the most important environmental factors contributing to lupus pathogenesis, exposure to ultraviolet B light (UVB) plays a critical role in inducing skin disease and can also promote systemic involvement (4). Due to the depth at which UVB penetrates the skin, keratinocytes are the most affected cell type, undergoing apoptosis. In lupus, an excessive apoptotic burden, perhaps with aberrant antigen presentation, can promote the generation of autoantibodies and formation of immune complexes. Immune complexes stimulate the production of many inflammatory cytokines, while influencing trafficking of immune cells (4,10).

One cytokine implicated in the pathogenesis of cutaneous lupus is TNF-like weak inducer of apoptosis (TWEAK; TNFSF12), a soluble cytokine that signals through its sole receptor, fibroblast growth factor inducible 14 (Fn14). TWEAK plays a role in many important cellular processes including angiogenesis, proliferation, cell death, and inflammation. We previously demonstrated that MRL/lpr mice that lack Fn14 have ameliorated kidney (11) and brain disease (12). This same protection extends to the skin as well, as MRL/lpr Fn14 knockout (Fn14KO) mice have attenuated skin lesions (13). The architecture of the skin of MRL/lpr Fn14KO mice was well maintained, whereas Fn14 wildtype (Fn14WT) mice displayed epidermal thickening and disruption of the dermo-epidermal junction. Mechanistically, ameliorated disease in MRL/lpr Fn14KO mice could be partly attributed to attenuation of chemokine expression and decreased apoptosis. Keratinocytes stimulated with TWEAK produce RANTES, in an Fn14-dependent manner; and also have enhanced apoptosis, *in vivo* and *in vitro* (13,14).

A possible role of Fn14 in lupus-associated photosensitivity has not been studied. Since both Fn14 and UVB promote apoptosis and an inflammatory milieu, we hypothesized that Fn14 signaling is involved in UVB-induced acute skin inflammation and injury. The primary purpose of this study was therefore to evaluate whether the TWEAK/Fn14 signaling axis

Author Manuscript Author Manuscript Author Manuscript Author Manuscript

participates in the development of UVB irradiation-induced skin lesions in autoimmune-prone MRL/lpr mice.

Materials and methods

Animals

Female MRL/lpr Fn14KO (ninth generation) and WT littermates (14–15 wk) were maintained at the Albert Einstein College of Medicine (15). Background strain control MRL/MpJ mice (10–12 wk) were from Jackson Laboratories. The institutional animal care committee approved all animal study protocols.

UVB irradiation

24 hours before irradiation, MRL/lpr Fn14WT and KO mice (13–15 wk) were shaved with clippers to remove the hair from their flank. Mice were anesthetized and placed in a cabinet fitted with a UVB lamp (UVM-57, UVP) and blocking any extraneous light sources. The head and hindlimb regions were protected using black Perspex. Mice received two doses of irradiation (50 mJ/cm^2), 24 hours apart, and were sacrificed 24 hours after the last dose (16,17). The same procedure was carried out for experiments involving MRL/lpr and MRL/MpJ mice (10–12 wk).

Histology scoring

Sections were blindly scored using a system adapted from Darr et al (18). Sections were given two scores; one for the epidermis (0–5, in increments of 0.5), which looked at the presence of sunburn cells, severity of interface dermatitis, and thickening of the epidermis, and one for the dermis (0–3, in increments of 0.5), which accounted for the amount of infiltrating cells. These scores were added together for a total score for each mouse (range 0–8; Supplemental Figure 1).

Fn14 flow cytometry

MRL/lpr mice (10 wk) were UVB-irradiated as above, and sacrificed 24 hours after the second exposure. Skin was minced, placed in 1× Tyrodes buffer, 2 mg/ml liberase (Sigma), and 15% BSA, and digested with gentle agitation at 37°C. After the incubation, the buffer mixture was removed to a new tube, carefully leaving the skin behind. The same buffer was added to the skin for a second digestion, combined with that from the first digestion, and strained into a tube containing FBS. A final mixture of Tyrodes buffer and 0.025% trypsin was added to the skin, incubated at 37°C, strained into the tube with FBS, and centrifuged. Cells were incubated with an Fn14-specific Fab'$_2$ (derived from P4A8) (19) or a control Fab'$_2$ MOPC-21 for 30 minutes. Cells were washed three times, and flow cytometry performed on a LSR II instrument. To induce apoptosis with staurosporine, PAM212 keratinocytes were treated with 10 μM staurosporine for 6 and 24 hours. Cells were then stained and analyzed as above.

Author Manuscript Author Manuscript Author Manuscript Author Manuscript

Histopathology, immunohistochemistry, and immunofluorescence

Tissue samples were immersed in 10% buffered formalin for 48 hours at 4°C, paraffin embedded, and stained using hematoxylin and eosin. For immunohistochemical staining with anti-CD3 (Fisher) following the addition of substrate solution, slides were rinsed in ddH20, stained in Mayer's hematoxylin, washed, air-dried, and mounted. Individual CD3+ cells were counted using ImageJ. For immunofluorescence, staining reagents included antibodies to IBA-1 (Wako), NGAL (R&D), and TUNEL (Roche). Following the addition of secondary antibodies, slides were stained with DAPI, washed, air-dried, and mounted. Images were taken on a Zeiss Axio Observer and quantified using ImageJ; intensity was determined for IBA-1 and NGAL because individual cell counts were less accurate using this staining method.

NGAL ELISA

Snap-frozen skin sections from UVB-irradiated mice were homogenized in T-PER tissue protein extraction buffer (Thermo) and centrifuged. Supernatants were collected and analyzed using a mouse NGAL duo-set ELISA kit (R&D).

Macrophage depletion

MRL/lpr mice (8 weeks of age) received 100 mg/kg of GW2580 (LC Laboratories) via oral gavage for 16 days. On the last two days of drug administration, mice were irradiated as described above and sacrificed 24 hours after the last dose of UVB. Macrophage depletion was confirmed by flow cytometry at multiple time-points (data not shown). Studies in normal rats noted no histological changes in a wide variety of tissues, including skin, upon GW2580 administration (20).

RNA isolation and RT-PCR

RNA isolation, reverse transcription, and real-time PCR (in triplicate) was performed as described previously. The genes of interest were normalized to the average of GAPDH and tubulin, and fold changes were determined using the delta-delta CT method (13).

Multiplex chemokine array

Snap-frozen skin from irradiated mice and control mice was homogenized in T-PER tissue protein extraction buffer (Thermo) and centrifuged. Protein concentrations were normalized, and chemokine concentrations analyzed using the LEGENDPlex Mouse Proinflammatory Chemokine Panel (Biolegend).

Analysis

The results shown are mean±SE. For the immunofluorescent and immunohistochemical staining studies, multiple fields were evaluated per mouse (CD3, n=9; IBA-1, n=5; NGAL, n=6; TUNEL, n=4). The mean was then used as the assigned value for that particular mouse when calculating the differences between the genotypes. Values of $P<0.05$ were considered significant.

Author Manuscript Author Manuscript Author Manuscript Author Manuscript

Results

Fn14 deficiency protects MRL/lpr mice from effects of UVB

To assess the contribution of the TWEAK/Fn14 signaling axis to the pathogenesis of photosensitivity and UVB-accelerated disease, we UVB-irradiated MRL/lpr Fn14WT and Fn14KO mice and assessed the histopathology 24 hours following two doses of UVB. Non-UVB exposed skin from the same mice served as a control. Following UVB irradiation, MRL/lpr Fn14KO mice show decreased hyperkeratosis, parakeratosis, disruption of the dermo-epidermal junction, and sunburn cells, as compared to Fn14WT mice (Figure 1a, left). Histological analysis of skin sections (scored blindly) showed that MRL/lpr Fn14KO have significantly less severe cutaneous damage as compared to Fn14WT mice (mean skin score 2.45±0.32 vs 3.84±0.42, respectively; p=0.009) (Figure 1a, right; Supplemental Figure 2). UVB irradiation did not lead to any differences in systemic manifestations, including ssDNA or dsDNA antibody levels, between MRL/lpr Fn14WT and KO mice (data not shown).

UVB irradiation leads to upregulation of Fn14 on apoptotic cells

While Fn14 is basally expressed in the skin and elsewhere (21,22), its expression, in general, significantly increases following tissue insult or injury. Previously we found upregulation of Fn14 in keratinocytes in response to UVB *in vitro*. To confirm the *in vivo* relevance of this observation, single cells were isolated from the skin of MRL/lpr mice following irradiation to determine the effect of UVB on Fn14 expression. UV-irradiated MRL/lpr mice had increased Fn14+ cells in the early apoptotic (7-AAD-/annexin-V+) population when compared to those that were not irradiated (16.38±0.63 vs 11.41±0.71, p=0.0008). A similar upregulation of Fn14 was also seen in the late apoptotic (7-AAD+/annexin-V+) fraction (UV=74.36±2.05, no UV=44.36±7.18, p=0.004) (Supplemental Figure 3a). Fn14 upregulation was also seen on keratinocytes treated with staurosporine (Supplemental Figure 3b). This latter observation suggests that upregulation of Fn14 following an apoptotic stimulus is not UV-specific, but can occur in keratinocytes undergoing apoptosis in response to other triggers as well. Fn14 upregulation in keratinocytes in response to UVB was also confirmed by immunohistochemistry of intact skin (data not shown).

UVB-treated MRL/lpr Fn14KO mice show decreased skin apoptosis and fewer infiltrating T cells

UVB is involved in the pathogenesis of cutaneous lupus through both its proapoptotic and proinflammatory effects (4,10). To analyze for the presence of apoptotic cells in irradiated skin, we used TUNEL staining. Staining was significantly less pronounced in the epidermis of MRL/lpr Fn14KO mice compared to Fn14WT mice (3.77±0.70 vs 9.08±1.48, respectively; p= 0.02) (Figure 1b). To assess the types of immune cells infiltrating the skin following UVB, immunohistochemistry were performed. Following irradiation, MRL/lpr Fn14KO mice had fewer infiltrating T cells as compared to MRL/lpr Fn14WT mice (average cell count in 20× fields: 6.21±1.13 vs 11.20±1.14, respectively; p= 0.009) (Figure 1c). Non-UVB exposed skin from MRL/lpr Fn14 WT and KO mice showed no infiltration with CD3+ cells (data not shown).

Author Manuscript Author Manuscript Author Manuscript Author Manuscript

UVB irradiation induces NGAL production in the skin

Lipocalin-2 (LCN2 or neutrophil gelatinase-associated lipocalin, NGAL) is a protein, first described in neutrophils, that is upregulated in inflammatory conditions in both macrophages and keratinocytes (23,24). Neutrophils have been implicated in CLE pathogenesis (10), and increased epidermal neutrophils are seen in patients exposed to UVB (25). NGAL can affect macrophage polarization and activation (23), and has also been shown to regulate levels of both Fn14 and TWEAK, thus influencing breast cancer invasiveness (26). Furthermore, NGAL can play a role in adaptive immunity (27). We therefore investigated the levels of NGAL following UVB irradiation. MRL/lpr mice showed increased expression of NGAL in the skin following UVB irradiation, whereas levels in MRL/MpJ mice were unchanged (Figure 2a). However, MRL/lpr Fn14KO mice had decreased NGAL levels in response to UVB compared to Fn14WT mice (Figure 2b). Furthermore, immunofluorescence studies confirmed that MRL/lpr Fn14KO mice had decreased NGAL+ cells infiltrating the skin following UVB exposure as compared to Fn14WT mice (0.89±0.23 vs 1.95±0.26, p= 0.007) (Figure 2c). Non-UVB exposed skin from MRL/lpr Fn14 WT and KO mice did not stain positive for NGAL (data not shown).

Macrophage depletion protects MRL/lpr mice from effects of UVB irradiation

Exposing lupus-prone mice to UVB elicits the production of CSF-1 by keratinocytes; it was hypothesized that CSF-1 then in turn recruits macrophages to areas of inflammation in the skin, where they can secrete mediators that promote apoptosis (9). Furthermore, we and others have previously shown that Fn14 signaling in keratinocytes induces chemokines that may promote macrophage recruitment (13,14). We found that MRL/lpr Fn14KO mice had fewer infiltrating IBA-1+ macrophages after UVB when compared to Fn14WT mice (percent area; 2.69±0.69 vs 5.49±0.64, respectively; p=0.008) (Figure 3a; Supplemental Figure 4a). Importantly, the number of IBA-1+ cells infiltrating lesional skin correlated with histology scores ($r = 0.96$, $p<0.0001$; data not shown).

Macrophages may also express the Fn14 receptor (28,29). Moreover, in previous studies we found that depletion of macrophages using a CSF-1R specific kinase inhibitor, GW2580, is protective against the development of lupus nephritis (30). To determine whether the beneficial effects of Fn14 deficiency following UVB exposure of lupus mice are indeed mediated by macrophages, we depleted macrophages using this same pharmacological approach. Control treated MRL/lpr mice that were subsequently irradiated displayed marked skin injury, including sunburn cells and hyperkeratosis (Figure 3b, left panel). In contrast, MRL/lpr mice treated with GW2580 at a dose which we previously showed depletes macrophages/monocytes from the spleen and circulation were significantly protected from development of cutaneous lesions (mean skin scores of 2.63±0.18 vs 4.48±0.41 in control treated mice; p=0.004) (Figure 3b; Supplemental Figure 4b), directly confirming a pathogenic role for macrophages in UVB-induced cutaneous lupus. GW treatment alone, without UVB, did not elicit histopathological skin changes (data not shown). Importantly, GW2580 treatment did not affect the levels of NGAL, suggesting that this molecule is being produced by neutrophils, not macrophages (data not shown). Next, we explored whether the contribution of infiltrating macrophages to the development of cutaneous lesions in UVB-irradiated mice is dependent on Fn14 expression by depleting macrophages in MRL/lpr

Author Manuscript Author Manuscript Author Manuscript Author Manuscript

Fn14WT and KO mice. MRL/lpr Fn14WT mice had improved cutaneous histology following depletion with GW2580, versus control treatment (p-value=0.02) (Figure 3c; Supplemental Figure 4c), whereas in Fn14KO mice there was no further attenuation with macrophage depletion (data not shown).

UVB irradiation leads to increased chemokine production

We studied chemokine production in the skin of UVB-irradiated and control mice. There was increased mRNA expression of several chemokines in irradiated mice (all data provided as fold change of UV versus control mice): MIP1α (21.09±2.11 vs 1.68±0.93, p-value <0.0001), CXCL1 (6.14±0.35 vs 1.28±0.40, p-value <0.0001), and CXCL5 (40.99±10.36 vs 1.45±0.49, p-value = 0.005) (Figure 4).

Measuring actual protein concentrations in skin lysates, we found that UV exposure led to increased production of the same chemokines when compared to unmanipulated mice, including MCP-1 (3.92±0.43 vs 1.55±0.29 pg/ml, p=0.004), MIP1α (295.0±47.73 vs 27.07±9.73 pg/ml, p=0.002), CXCL1 (43.46±6.43 vs 8.78±2.11 pg/ml, p=0.002), and CXCL5 (58.48±17.28 vs 5.46±0.87 pg/ml, p=0.02) (Figure 4). MIP3α and RANTES showed similar trends (data not shown). Furthermore, we found that MIP1α and MIP1β were significantly upregulated in the skin of irradiated MRL/lpr Fn14WT as compared to Fn14KO mice (Supplemental Figure 5). Finally, this study also confirmed the downregulation of macrophage related genes in GW2580 treated mice (Supplemental Figure 5).

Discussion

We found that the TWEAK receptor, Fn14, is instrumental in the development of cutaneous disease following acute UVB exposure, as MRL/lpr Fn14KO mice develop significantly less severe skin lesions. Given the acute nature of the experimental protocol, features of both CLE and UVB damage were noted. Classic features found in UVB irradiated skin (24 hours following exposure) include thickening of the stratum corneum, epidermal spongiosis, microvesicles/pustules, sunburn cells, and superficial vascular dilatation (31,32). While these features were seen in both Fn14WT and KO mice, the severity was significantly enhanced in WT. Primary histologic features of acute CLE include basal vacuolar interface dermatitis and a papillary dermal perivascular lymphocytic infiltrate. Findings such as follicular plugging, epidermal atrophy, and colloid bodies can be seen as well, but are more often associated with chronic cutaneous lupus lesions (33). We found that UVB exposed MRL/lpr Fn14 WT, but not KO mice, demonstrated several typical features of cutaneous lupus, including interface dermatitis, in some cases associated with subepidermal clefting resulting from the basilar degeneration. Moreover, several sections demonstrated numerous necrotic basal keratinocytes in conjunction with the interface dermatitis. Furthermore, a peri-adnexal and lobular lymphocytic infiltrate, and follicular plugging, was seen only in the irradiated Fn14WT but not KO mice. Taken together, these findings are strongly supportive of the induction of evolving CLE (albeit in conjunction with a contribution of UVB induced damage) in UVB challenged lupus-prone MRL/lpr Fn14 wildtype mice, while such features were significantly attenuated or absent in Fn14KO mice.

Author Manuscript Author Manuscript Author Manuscript Author Manuscript

Our previous studies attributed ameliorated spontaneous disease in MRL/lpr Fn14KO mice to abrogated TWEAK-induced chemokine production by keratinocytes, as well as decreased levels of keratinocyte apoptosis. We have now shown that UVB-dependent upregulation of Fn14 also triggers immune cell infiltration *in vivo*, as MRL/lpr Fn14KO mice have fewer infiltrating T cells, macrophages, and NGAL+ cells following UVB exposure. In addition, overexpression of Fn14 following UVB could allow for increased interactions with TWEAK in the tissue, leading to a positive feedback loop involving chemokine upregulation and further cellular recruitment. UVB-triggered upregulation of Fn14 may have other effects as well; it can lead to increased apoptosis as shown here in MRL/lpr Fn14WT mice, and could also contribute to increased sensitivity of keratinocytes to a combination of TWEAK+UVB, demonstrated previously *in vitro* (13). Additional novel observations in this study concern the role of innate immunity in the pathogenesis of photosensitive skin lesions in lupus, as seen in the conclusive linkage of macrophages to the pathogenesis and the possible contribution of NGAL to the local inflammatory milieu in MRL/lpr mice following UVB exposure.

TWEAK/Fn14 mediated apoptosis factors in several different dermatologic conditions, both neoplastic and inflammatory. Studies in melanoma lines and primary cells showed overexpression of Fn14 compared to normal melanocytes. When melanoma cells were treated with an Fn14-specific immunotoxin, cell death resulted via multiple signaling pathways (34). Nakayama et al also described TWEAK-induced cell death in tumor cell lines, including squamous cell carcinoma. The ITEM-4 anti-Fn14 antibody was able to block these cytotoxic effects, thereby suggesting that Fn14 is key to the process of cell death (35). As for inflammatory skin disease, both TWEAK and Fn14 are upregulated in psoriatic lesions and lesional skin biopsies from patients with atopic dermatitis (36). The latter study also demonstrated that TWEAK induces apoptosis in human keratinocytes *in vitro* (36).

Studies have further closely examined the association between the induction of apoptosis and Fn14 expression. Stressing osteoblasts by mechanical stretching led to an increase in Fn14 mRNA and activation of caspase 3. Levels of Fn14 decreased after removal of the stressor; therefore, degradation of Fn14 may negatively regulate Fn14-induced apoptosis (37). Studies in cerebral ischemia have shown that oxygen-glucose deprivation leads to upregulation of Fn14 mRNA (38). Previous findings indicate that stress induced Fn14 upregulation was operative also in skin cells, specifically keratinocytes, following exposure to UVB *in vitro* (13). Importantly, in the present study we were able to demonstrate UVB-induced Fn14 regulation in lupus skin *in vivo* as well, with keratinocytes upregulating surface Fn14 expression following irradiation. We believe that keratinocytes, and possibly other cell types in the skin as well as well, become stressed and upregulate Fn14, sensitizing them to TWEAK and subsequently leading to apoptosis. In the context of the attenuated disease seen in Fn14 deficient mice, such sensitization would not occur due to the lack of the receptor. Although for technical reasons related to strain availability we did not directly show which cells upregulated Fn14 in skin tissue lysates, our previous data in the PAM212 keratinocytes, the sensitivity of keratinocytes to irradiation, the proximity of these cells to the source of irradiation, and the staining results in irradiated intact tissue all indicate that the primary cells upregulating Fn14 in the skin following UVB exposure are keratinocytes.

Author Manuscript Author Manuscript Author Manuscript Author Manuscript

Following irradiation, MRL/lpr keratinocytes produce CSF-1 which can direct recruitment of monocytes to the skin, where they can then secrete proinflammatory cytokines and induce keratinocyte apoptosis (9). We found infiltrating IBA-1+ macrophages in MRL/lpr Fn14WT lesional skin following UVB. While these cells are still present in the lesions of Fn14KO mice, their numbers were significantly reduced. We also found that depletion of macrophages using GW2580 led to protection from the development of lesions, confirming a previously unrecognized pathogenic role for these cells in UVB-induced disease. T cells have also been implicated in CLE pathogenesis; CD4 and CD8 cells are deposited at the dermo-epidermal junction, elevated amounts of Th17 cells are present, and decreased levels of Tregs are found in skin lesions (39). We also observed increased T cells infiltrating the skin after UVB exposure. Similar to macrophages, T cells are found in irradiated Fn14KO mice, but in lesser numbers as compared to Fn14WT. Presumably, the reduction of infiltrating cells in Fn14KO is due to decreased levels of TWEAK-induced chemokines. A similar phenomenon was present following induction of renal disease by nephrotoxic serum transfer, where MCP-1 and VCAM-1 were downregulated in kidneys of Fn14 KO as compared to WT mice (40).

NGAL, which is expressed by both macrophages and neutrophils, has been identified as a marker of acute and chronic kidney injury. The pathophysiological role of NGAL is not completely understood, however, showing both model-dependent protective or pathogenic effects. NGAL has an anti-inflammatory role and can “deactivate” macrophages, suppressing immune responses (23,41). Models of *E. coli* and *Mycobacteria* infection result in high levels of NGAL, which can limit bacterial growth (42). In contrast, a pathogenic role for NGAL is seen in nephritis, with ameliorated disease in NGAL knockout mice following nephrotoxic serum transfer. Kidney NGAL expression increases as a result of autoantibody binding; this facilitates further inflammation because it leads to apoptosis of resident cells and chemokine induction (27). Following stimulation by UVB, we found an increase in NGAL+ cells infiltrating lesional skin. MRL/lpr Fn14KO mice have fewer of these cells and their skin lesions are less severe, therefore suggesting a novel pathological role for these NGAL+ cells in UVB-induced lesions.

Finally, we found that irradiation led to increased levels of proinflammatory chemokines in the skin, at both the mRNA and protein level. Molecules such as CXCL5, CXCL1, and MIP1α, produced by macrophages and chemoattractant for cells such as T cells and neutrophils, are hyperexpressed in irradiated as compared to non-exposed skin. Additionally, we found that some of these proinflammatory mediators, including MIP1α and MIP1β, were decreased in the skin following GW2580 treatment, further supporting the importance of macrophages and the contributions of chemokines to skin lesion development. Moreover, MIP1α and MIP1β were decreased in irradiated MRL/lpr Fn14 KO mice compared to Fn14 WT mice, suggesting regulation through Fn14. Thus, we show regulation of chemokine production via TWEAK/Fn14 signaling in the context of UVB irradiation, which has not been previously explored. It is nevertheless important to acknowledge that at least some of the UVB induced inflammatory mediators (e.g. CXCL1, CXCL5) are not specific to a CLE-like inflammatory process, but can also be upregulated by UVB-induced skin injury.

Author Manuscript Author Manuscript Author Manuscript Author Manuscript

In this study, we demonstrate the centrality of signaling via Fn14 in the pathogenesis of UV-accelerated cutaneous lupus. We found that UVB exposure upregulates Fn14 on skin cells undergoing apoptosis. In UVB-irradiated MRL/lpr mice, skin cells then also become more sensitized to the effects of TWEAK, resulting in increased keratinocyte apoptosis and the production of inflammatory chemokines. Subsequently, increased numbers of T cells, macrophages, and NGAL+ cells traffic to the skin in response to the chemotactic gradient. Moreover, histology scores significantly correlated with the number of infiltrating macrophages and NGAL+ positive cells. Confirming that macrophages are pathogenic in UVB-accelerated cutaneous injury distal to Fn14 signaling, depletion of macrophages is protective in Fn14WT but not Fn14KO MRL/lpr mice. Thus, skin disease is significantly attenuated in UVB exposed MRL/lpr Fn14KO mice, mostly due to the lack of TWEAK-induced chemokine production, decreased infiltration by inflammatory cells including macrophages, and reduced apoptosis. With this data we conclude that TWEAK/Fn14 is critical in the pathogenesis of UVB-induced lesions in lupus-prone mice. These findings have potentially important clinical relevance since we have previously demonstrated Fn14 upregulation in lesional and non-lesional skin from human lupus patients (13). Future studies will allow us to determine if this signaling axis participates more broadly in UVB-induced skin injury in humans, also outside the setting of autoimmunity.

Supplementary Material

Refer to Web version on PubMed Central for supplementary material.

Acknowledgments

This study was supported by grants from the NIH AR048692 and AR065594 (to CP). We thank Dr. Nancy Bigley (Wright State University) for PAM212 keratinocytes, and the Einstein Histopathology Core Facility for assistance in immunohistochemical staining. MRL/lpr Fn14WT and KO mice were a kind gift from Dr. Linda Burkly (Biogen Idec).

Abbreviations

CLE	cutaneous lupus erythematosus
KO	knockout
SLE	systemic lupus erythematosus
STS	staurosporine
TWEAK	TNF-like weak inducer of apoptosis
UV	ultraviolet
UVB	ultraviolet B
WT	wild-type

References

1. Tsokos GC. N Engl J Med. 2011; 365:2110–2121. [PubMed: 22129255]

Author Manuscript Author Manuscript Author Manuscript Author Manuscript

2. Okon LG, Werth VP. Best Pract Res Clin Rheumatol. 2013; 27:391–404. [PubMed: 24238695]
3. Lin JH, Dutz JP, Sontheimer RD, et al. Clin Rev Allergy Immunol. 2007; 33:85–106. [PubMed: 18094949]
4. Kuhn A, Wenzel J, Weyd H. Clin Rev Allergy Immunol. 2014; 47:148–62. [PubMed: 24420508]
5. Oke V, Wahren-Herlenius M. J Intern Med. 2013; 273:544–554. [PubMed: 23464352]
6. Cohen PL, Eisenberg RA. Annu Rev Immunol. 1991; 9:243–269. [PubMed: 1910678]
7. Furukawa F, Yoshimasu T. Autoimmun Rev. 2005; 4:345–350. [PubMed: 16081025]
8. Ghoreishi M, Dutz J. Lupus. 2010; 19:1029–1035. [PubMed: 20693196]
9. Menke J, Hsu M-Y, Byrne KT, et al. J Immunol. 2008; 181:7367–7379. [PubMed: 18981160]
10. Achtman JC, Werth VP. Arthritis Res Ther. 2015; 17:182. [PubMed: 26257198]
11. Xia Y, Herlitz LC, Gindea S, et al. J Am Soc Nephrol. 2015; 26:1053–1070. [PubMed: 25270074]
12. Wen J, Xia Y, Stock A, et al. J Autoimmun. 2013; 43:44–54. [PubMed: 23578591]
13. Doerner JL, Wen J, Xia Y, et al. J Invest Dermatol. 2015; 135:1986–1995. [PubMed: 25826425]
14. Jin L, Nakao A, Nakayama M, et al. J Invest Dermatol. 2004; 122:1175–1179. [PubMed: 15140220]
15. Jakubowski A, Ambrose C, Parr M, et al. J Clin Invest. 2005; 115:2330–2340. [PubMed: 16110324]
16. Matsuda M, Hoshino T, Yamashita Y, et al. J Biol Chem. 2010; 285:5848–5858. [PubMed: 20018843]
17. Schäfer M, Dütsch S, auf dem Keller U, et al. Genes Dev. 2010; 24:1045–1058. [PubMed: 20478997]
18. Darr D, Dunston S, Faust H\, et al. Acta Derm Venereol. 1996; 76:264–268. [PubMed: 8869680]
19. Michaelson JS, Amatucci A, Kelly R, et al. MAbs. 2011; 3:362–375. [PubMed: 21697654]
20. Conway JG, Pink H, Bergquist ML, et al. J Pharmacol Exp Ther. 2008; 326:41–50. [PubMed: 18434589]
21. Zimmermann M, Koreck A, Meyer N, et al. J Allergy Clin Immunol. 2011; 127:200–207.e10. [PubMed: 21211655]
22. Burkly LC, Michaelson JS, Zheng TS. Immunol Rev. 2011; 244:99–114. [PubMed: 22017434]
23. Guo H, Jin D, Chen X. Mol Endocrinol. 2014; 28:1616–1628. [PubMed: 25127375]
24. Borregaard N, Sørensen OE, Theilgaard-Mönch K. Trends Immunol. 2007; 28:340–345. [PubMed: 17627888]
25. Janssens AS, Lashley EELO, Out-Luiting CJ, et al. Exp Dermatol. 2005; 14:138–142. [PubMed: 15679584]
26. Gaudineau B, Fougère M, Guaddachi F, et al. J Cell Sci. 2012; 125:4475–4486. [PubMed: 22767506]
27. Pawar RD, Pitashny M, Gindea S, et al. Arthritis Rheum. 2012; 64:1620–1631. [PubMed: 22083497]
28. Sanz AB, Aroeira LS, Bellon T, et al. PLoS ONE. 2014; 9:e90399. [PubMed: 24599047]
29. Molano A, Lakhani P, Aran A, et al. Immunol Lett. 2009; 125:119–128. [PubMed: 19573558]
30. Chalmers SA, Chitu V, Herlitz LC, et al. J Autoimmun. 2015; 57:42–52. [PubMed: 25554644]
31. Avila Acevedo JG, Espinosa González AM, De Maria y Campos DM, et al. BMC Complement Altern Med. 2014; 14:281. [PubMed: 25086781]
32. Ulrich M, Rüter C, Astner S, et al. Br J Dermatol. 2009; 161(Suppl 3):46–53. [PubMed: 19775357]
33. Obermoser G, Sontheimer RD, Zelger B. Lupus. 2010; 19:1050–1070. [PubMed: 20693199]
34. Zhou H, Ekmekcioglu S, Marks JW, et al. J Invest Dermatol. 2013; 133:1052–1062. [PubMed: 23190886]
35. Nakayama M, Ishidoh K, Kojima Y, et al. J Immunol. 2003; 170:341–348. [PubMed: 12496418]
36. Sabour Alaoui S, Dessirier V, de Araujo E, et al. PLoS ONE. 2012; 7:e33609. [PubMed: 22438963]
37. Matsui H, Fukuno N, Kanda Y, et al. J Biol Chem. 2014; 289:6438–6450. [PubMed: 24446436]
38. Haile WB, Echeverry R, Wu F, et al. Neuroscience. 2010; 171:1256–1264. [PubMed: 20955770]

Author Manuscript Author Manuscript Author Manuscript Author Manuscript

39. Yu C, Chang C, Zhang J. J Autoimmun. 2013; 41:34–45. [PubMed: 23380467]
40. Xia Y, Campbell SR, Broder A, et al. Clin Immunol. 2012; 145:108–121. [PubMed: 22982296]
41. Eller K, Schroll A, Banas M, et al. PLoS ONE. 2013; 8:e67693. [PubMed: 23861783]
42. Li C, Chan YR. Cytokine. 2011; 56:435–441. [PubMed: 21855366]

Author Manuscript Author Manuscript Author Manuscript Author Manuscript

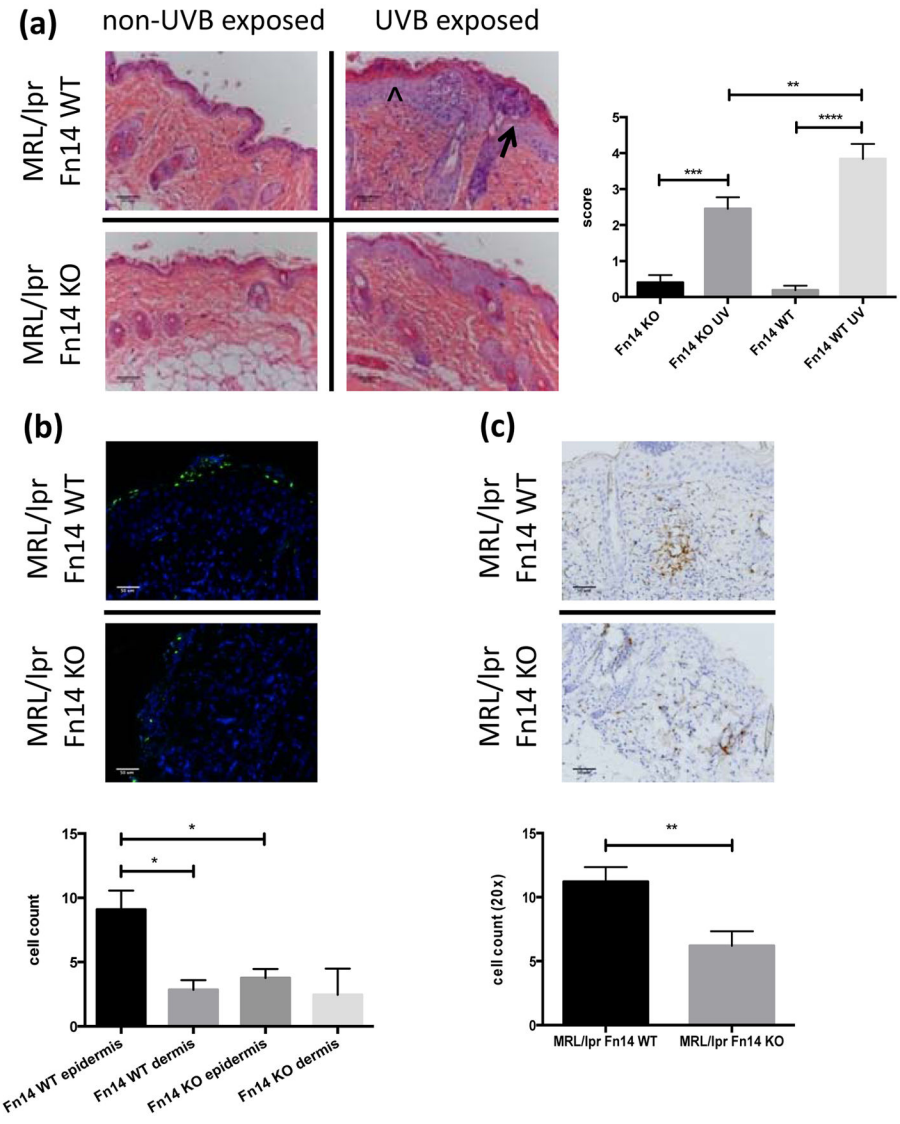

Figure 1.

Fn14 deficient MRL/lpr mice are less photosensitive. (a) Shown here are representative H&E images from UVB-exposed and non-exposed skin of MRL/lpr Fn14 WT and KO mice. The arrowhead represents acanthotic epidermis and the arrow points toward an epidermal pustule (left panel). Histopathological skin scores from 13–15 week old female UVB-irradiated MRL/lpr Fn14WT (n=14) and MRL/lpr Fn14KO mice (n=15) are shown in the right panel. (b) Representative images of TUNEL stained paraffin-embedded skin sections from UVB-irradiated MRL/lpr Fn14WT (n=6) and MRL/lpr Fn14KO mice (n=6) (top panel). TUNEL positive cells in the epidermis and dermis were counted using ImageJ (bottom panel). (c) Skin was obtained from UVB-exposed MRL/lpr Fn14 WT and KO mice. Shown are representative images of CD3 stained sections from randomly selected 13–15 week old female UVB-irradiated MRL/lpr Fn14WT (n=7) and MRL/lpr Fn14KO mice (n=7) skin. The bottom panel shows the quantitation of CD3 staining; cells were counted in

random 20× fields using ImageJ (WT, n=7; KO, n=7). The figures are representative of 2–3 independent experiments. *P<0.05, **P<0.01, ***P<0.001, ****P<0.0001.

Author Manuscript Author Manuscript Author Manuscript Author Manuscript

Author Manuscript Author Manuscript Author Manuscript Author Manuscript

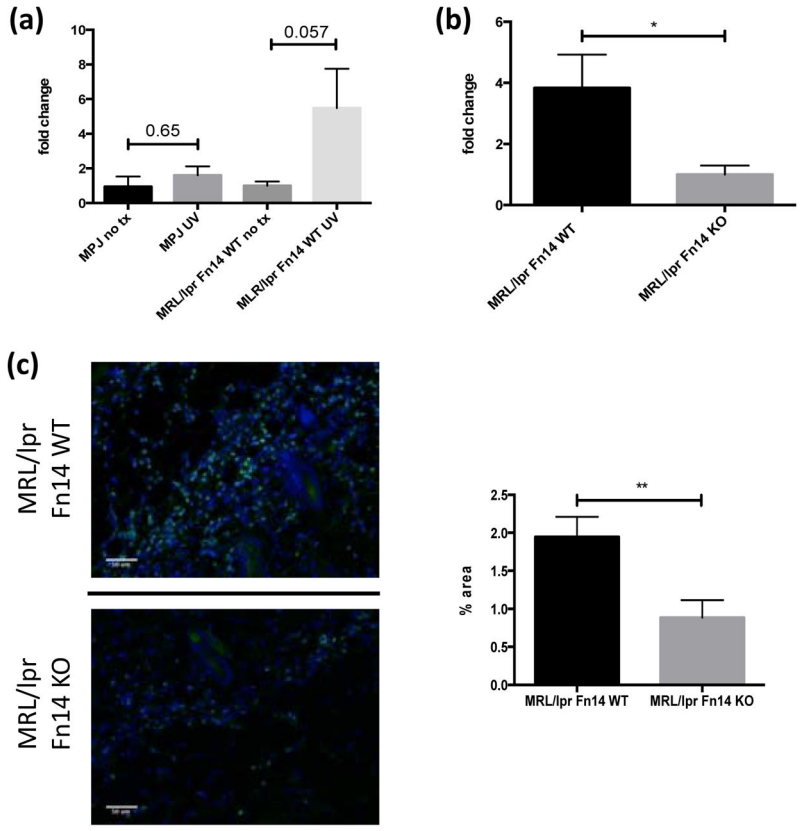

Figure 2.

UVB irradiation induces NGAL. (a) Nine to ten week old female MRL/lpr (n=4) and MRL/MpJ (n=4) mice were irradiated and skin lysates prepared as described above. Depicted in the graph are fold changes in NGAL concentrations compared to baseline, as measured by ELISA. The mean NGAL level in non-irradiated mice in each strain was arbitrarily set at 1. (b) Thirteen to fifteen week old female MRL/lpr Fn14WT (n=8) and Fn14KO (n=7) mice were irradiated, and NGAL in skin lysates analyzed as in (a). (c) Representative images of NGAL stained sections from randomly selected 13–15 week old female UVB-irradiated MRL/lpr Fn14WT (n=8) and Fn14KO mice (n=7). Quantitation of NGAL staining is provided in the right panel. The area with fluorescence was measured by ImageJ. **P*<0.05, ***P*<0.01.

Author Manuscript Author Manuscript Author Manuscript Author Manuscript

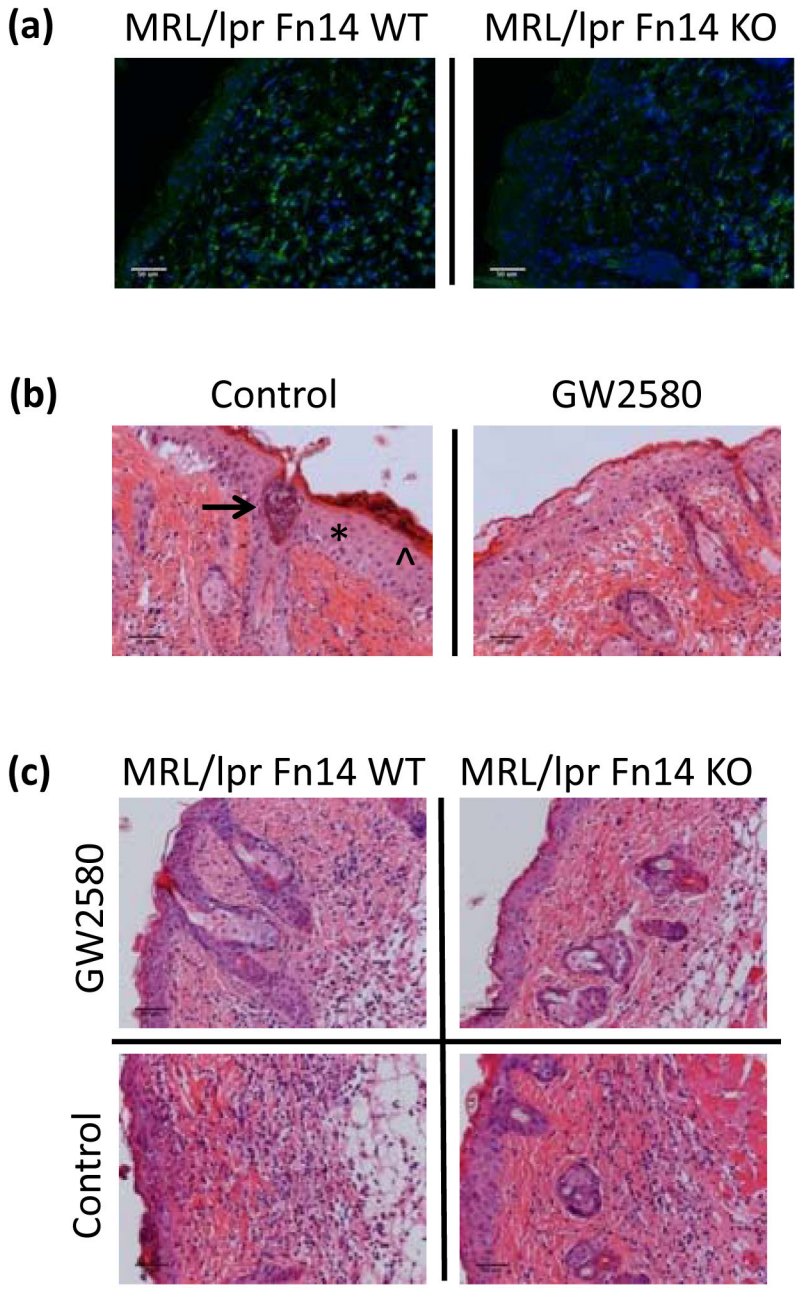

Figure 3.

Macrophage depletion protects MRL/lpr mice from UVB-induced injury. Skin was obtained from UVB-exposed and non-exposed MRL/lpr Fn14 WT and KO mice. (a) Shown are representative images of IBA-1 stained sections from randomly selected 13–15 week old female UVB-irradiated MRL/lpr Fn14WT (n=11) and MRL/lpr Fn14KO mice (n=10). (b) Eight week old female MRL/lpr mice were treated with GW2580 via oral gavage for 16 days. During the last two days of GW2580 treatment, mice were exposed to UVB (50 mJ/cm^2) and sacrificed 24 hours later. Shown are representative H&E images from GW (n=5) and PBS-treated (n=6) mice. The asterisk labels acanthotic epidermis, the arrowhead

Author Manuscript Author Manuscript Author Manuscript Author Manuscript

indicates parakeratosis, and the arrow points toward an epidermal pustule (left panel). (c) Representative H&E images of MRL/lpr Fn14WT (GW2580, n=3; PBS, n=2) and MRL/lpr Fn14KO mice (GW2580, n=3; PBS, n=2), treated and irradiated as above.

Author Manuscript Author Manuscript Author Manuscript Author Manuscript

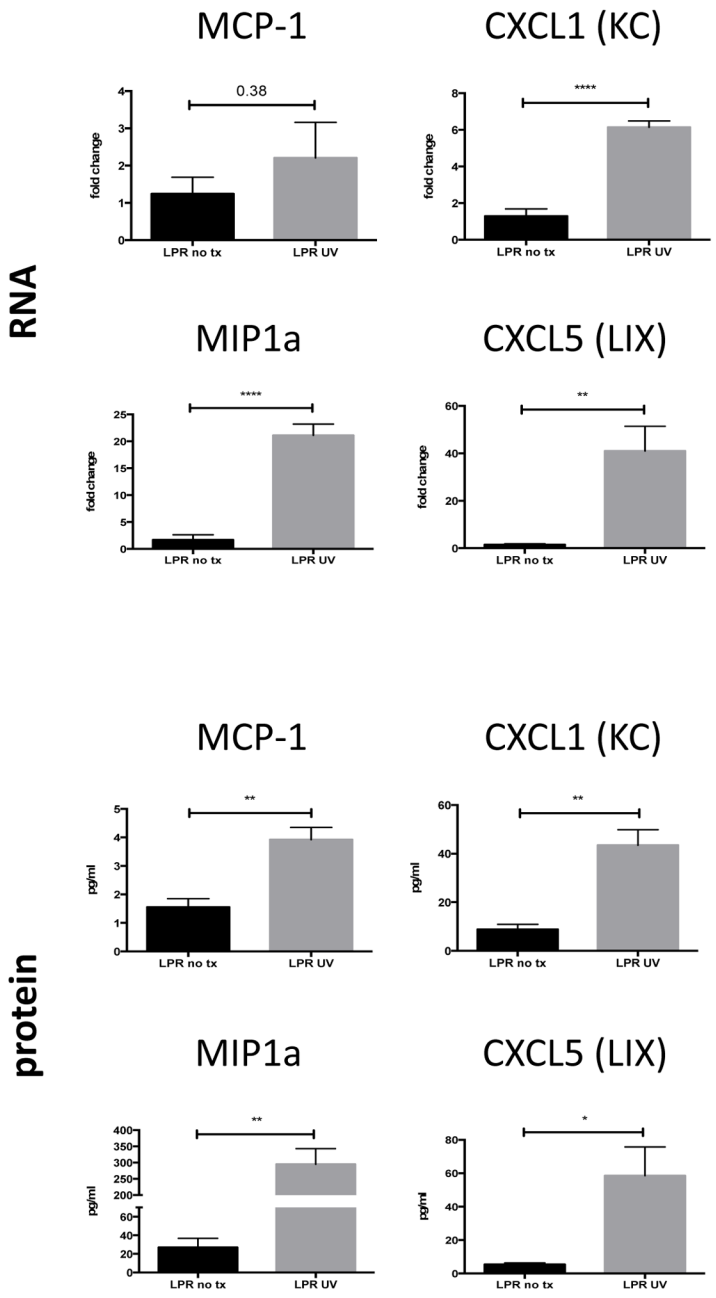

Figure 4.

UVB irradiation induces production of proinflammatory chemokines. Ten week old female MRL/lpr mice were irradiated as described above. RNA was isolated from irradiated mice (n=5) and unmanipulated controls (n=5), and analyzed for various chemokines by PCR (top panel). Chemokine levels in skin lysates from irradiated MRL/lpr mice (n=5) and unmanipulated MRL/lpr controls (n=4) were measured using a flow cytometer based multiplex assay (bottom panel). **P*<0.05, ***P*<0.01, *****P*<0.0001.